Translational Oncology
www.transonc.com

Volume 9 Number 4 August 2016 pp. 313–321 313

Global Conservation of Protein Status between Cell Lines and Xenografts[1]

Julian Biau[*,†,‡,§,¶,#], Emmanuel Chautard[¶,#], Frank Court[,††,‡‡], Bruno Pereira[§§], Pierre Verrelle[*,†,‡,¶,¶¶], Flavien Devun[*,##], Leanne De Koning[***] and Marie Dutreix[*,†,‡,§]**

*Institut Curie, Centre de Recherche, 91400 Orsay/75248 Paris, France; †UMR3347, Centre National de la Recherche Scientifique, 91400 Orsay, France; ‡U1021, Institut National de la Santé et de la Recherche Médicale, 91400 Orsay, France; §Université Paris Sud, 91400 Orsay, France; ¶Clermont Auvergne University, EA7283 CREaT, 63011 Clermont-Ferrand, France; #Radiotherapy Department, Centre Jean Perrin, 63011 Clermont-Ferrand, France; **U1103, Institut National de la Santé et de la Recherche Médicale, 63001 Clermont-Ferrand, France; ††UMR 6293, Centre National de la Recherche Scientifique, 63001 Clermont-Ferrand, France; ‡‡Clermont Auvergne University, GReD Laboratory, Clermont-Ferrand, 63000, France; §§Biostatistics Department, DRCI, Clermont-Ferrand Hospital, Clermont-Ferrand, 63003, France; ¶¶Radiotherapy Department, Institut Curie, 75005 Paris, France; ##DNA Therapeutics, Evry, Paris, France; ***Institut Curie, Department of Translational Research, RPPA platform,75248 Paris cedex05, France

Abstract

Common preclinical models for testing anticancer treatment include cultured human tumor cell lines in monolayer, and xenografts derived from these cell lines in immunodeficient mice. Our goal was to determine how similar the xenografts are compared with their original cell line and to determine whether it is possible to predict the stability of a xenograft model beforehand. We studied a selection of 89 protein markers of interest in 14 human cell cultures and respective subcutaneous xenografts using the reverse-phase protein array technology. We specifically focused on proteins and posttranslational modifications involved in DNA repair, PI3K pathway, apoptosis, tyrosine kinase signaling, stress, cell cycle, MAPK/ERK signaling, SAPK/JNK signaling, NFκB signaling, and adhesion/cytoskeleton. Using hierarchical clustering, most cell culture-xenograft pairs cluster together, suggesting a global conservation of protein signature. Particularly, Akt, NFkB, EGFR, and Vimentin showed very stable protein expression and phosphorylation levels highlighting that 4 of 10 pathways were highly correlated whatever the model. Other proteins were heterogeneously conserved depending on the cell line. Finally, cell line models with low Akt pathway activation and low levels of Vimentin gave rise to more reliable xenograft models. These results may be useful for the extrapolation of cell culture experiments to *in vivo* models in novel targeted drug discovery.

Translational Oncology (2016) 9, 313–321

Address all correspondence to: Julian Biau, 58 rue Montalembert, Département de Radiothérapie, Centre Jean Perrin, 63011 Clermont-Ferrand, France.
E-mail: Julian.biau@clermont.unicancer.fr
[1] Conflict of interest: none.
Received 19 March 2016; Revised 26 May 2016; Accepted 31 May 2016

1936-5233/16
http://dx.doi.org/10.1016/j.tranon.2016.05.005

Introduction

Developing a new drug from original idea to the launch of a finished product is a complex process which can take 12 to 15 years and costs more than $1 billion [1]. During lead discovery, an intensive search ensues to find a drug-like small molecule or biological therapeutic, typically termed a *development candidate*, that will progress into preclinical and, if successful, into clinical development and ultimately be a marketed medicine. Common preclinical models include cultured human tumor cell lines in monolayer, and xenografts derived from the same human lines in immunodeficient mice [2,3]. Monolayer cell cultures used in cancer biology and drug discovery are cost-effective and necessary for high-throughput screening but are generally highly reductionist (for its inability to capture the complexity and heterogeneity of a cancer) [4]. *In vivo* modeling provides essential tumor-host interactions and is a more accurate means of modeling human cancer in terms of toxicity and *in vivo* antitumor effectiveness. Its importance as models for drug testing and translational study has been recognized by many biomedical and pharmaceutical companies [5], and their validation and optimization are therefore essential. However, *in vivo* modeling has several drawbacks such as necessity of adapted structures and highly qualified personal or limitations on engraftment rates that might limit their applicability.

The features of models used in cancer research constitute critical tools for elucidating mechanisms of cancer development, as well as for assessment of putative cancer therapies. Although cell cultures studies allow a high-throughput screening, their major drawbacks, which make *in vivo* assessment necessary, are the lack of tumor microenvironment and the lack of heterogeneity observed in primary cancer [6]. Cell line xenograft models present only a murine stroma, and if subclones can coexist, primary cancer heterogeneity is probably lost. Nevertheless, animal models are necessary for preclinical research, and therefore, their validation and optimization are essential.

High-throughput screening approaches are largely used to characterize cell lines and tumors and identify biomarkers that could be associated to diagnosis or prognosis [7]. The most currently used analyzed the RNA content (transcriptome) or DNA modification (genome) through dedicated microarrays or, more recently, high-throughput sequencing. However, in mammalian species, most of the regulatory modifications occur at the level of proteins, and it is widely accepted that their amount and their posttranslational modifications regulate cell signaling pathways that govern cell behavior and their capacity to proliferate and escape from treatment [8,9]. Other posttranslational modifications and notably histone methylation and acetylation could also affect gene expression and therefore protein expression [10]. Moreover, whereas we do not expect major change in the genome of cells once they are grafted on mice, the (phospho-)proteome can evolve via the interaction with the microenvironment, the limit in oxygen and nutriments, and the signals exchange with the stroma [11–13]. These differences could account for discrepancies sometime reported between cell response to treatment and results *in vivo* [1,3]. However, despite the increasing interest for proteome, the methods to characterize it are still limited. Notably, the analysis of the phosphoproteome by mass spectrometry is promising but still very challenging [14] and requires large amounts of protein lysate (several mg) that are difficult to obtain from *in vivo* studies or patient samples [15]. In this study, we therefore used reverse-phase protein array (RPPA), a technology using high-throughput antibody-based detection. It requires only a few micrograms of protein lysate and allows assessing protein expression and their main modification status in a highly quantitative manner [9,16]. In contrast to mass spectrometry, this technology can analyze hundreds of samples simultaneously on the same array and thus generate large datasets to identify potential diagnostic, prognostic, and therapeutic markers in human cancer [17]. We applied this technology to a panel of 14 cell lines and their corresponding xenografts to assess how similar the xenografts are compared with their original cell line and to determine whether it is possible to predict the stability of a xenograft model beforehand. We explored a selection of proteins and modifications involved in 10 different signaling pathways: DNA repair, PI3K pathway, apoptosis, tyrosine kinase signaling, stress signaling, cell cycle, MAPK/ERK signaling, SAPK/JNK signaling, NFκB signaling, and adhesion/cytoskeleton.

Material and Methods

Cell Culture

Fourteen human cell lines were used: nine high-grade glioma cell lines (SF763, SF767, U251MG, U87MG, SNB19, MO59K, T98G, U118MG, and CB193), two colorectal cancer cell lines (HCT116 and HT29), two melanoma cell lines (SK28 and LU1205), and one head and neck cancer cell line (Hep-2). SF763, SF767, U251MG, and U87MG glioma cell lines were given by Dr. C. Delmas (Centre Claudius Regaud, Toulouse, France). U87MG cell line was used to obtain a U87MG-luciferase cell line (U87MG-L). SNB19 glioma cell line was given by N. Auger (Institut Curie, Paris, France). T98G, U118MG, and CB193 cell lines were kindly provided by G. Pennarun (CEA, Grenoble, France). MO59K and MO59J cell lines were given by N. Foray (Centre Léon Bérard, Lyon, France). HCT116, HT29, SK28, LU1205, and Hep-2 cell lines were obtained from ATCC (Manassas, VA). All culture reagents were purchased from GIBCO (Invitrogen, Cergy-Pontoise, France). Cells were grown in Dulbecco's modified Eagle's medium (with 4500 mg/l glucose and L-glutamine) supplemented with sodium pyruvate 1%, nonessential amino acids 1%, gentamicin 10 μg/ml, and 10% fetal calf serum in a humidified incubator containing 5% CO_2 at 37°C.

Xenograft Models

Xenografts derived from cell lines were obtained by injecting 4×10^6 cells of each cell line described above into the flank of adult female nude mice (Janvier, Le Genest Saint Isle, France). The animals were housed in our animal facility. There were six animals per cage under controlled conditions of light and dark cycles (12 hours: 12 hours), relative humidity (55%), and temperature (21°C). Food and tap water were available *ad libitum*. When subcutaneous tumors reached approximately 500 mm^3, mice were sacrificed. An anatomopathologist has evaluated the percentage of tumoral cells as being more than 80% for all cell line–based xenografts studied (using blind microscopy analysis of several samples per tumor). The Local Committee on Ethics of Animal Experimentation approved all experiments.

Antibodies and Validation

The 65 antibodies used are listed in Table S.1. We explored 39 total proteins and 26 phosphoproteins and then calculated 24 ratios of phosphoproteins on total proteins. These proteins and modifications were chosen as representative of 10 different signaling pathways: DNA repair, PI3K pathway, apoptosis, tyrosine kinase signaling, stress

signaling, cell cycle, MAPK/ERK signaling, SAPK/JNK signaling, NFκB signaling, and adhesion/cytoskeleton (Table S.1). To ensure that our antibodies were of sufficient quality, we confirmed their specificity by Western blotting on a large panel of cell lines treated with ligands and inhibitors. Antibodies with only a single or dominant band on Western blotting were validated and used in RPPA.

Preparation of Cell Lysates

Cell lines were scraped from plates in hot Laemmli buffer (50 mM Tris pH = 6.8, 2% SDS, 5% glycerol, 2 mM DTT, 2.5 mM EDTA, 2.5 mM EGTA, 2× Perbio Halt Phosphatase inhibitor cocktail, Roche Protease inhibitors complete MINI EDTA-free, 4 mM sodium orthovanadate, 20 mM sodium fluoride). Tumors were mechanically disrupted in the same lysis buffer (1 ml for 80 mg of sample) using a CK28 Precellys (Bertin Technologies, Montigny le Bretonneux, France) at 4°C, 6000 rpm, 60 seconds three times. Extracts were boiled for 10 minutes at +100°C and spinned for 15 minutes at 13,000 rpm at 15°C. The protein fraction was transferred to a new tube and spinned again at 13,000 rpm for 5 minutes at 15°C. The pellet was discarded, and lysates were snap-frozen. Protein concentration was measured using the Reducing Agent Compatible BCA kit (Pierce, Rockford, IL).

Reverse-Phase Protein Array

Proteins from 14 cell lines were analyzed with 5 replicates for cell cultures and 6 replicates for subcutaneous xenograft models (2 different locations in 3 different tumors per model). Samples were printed onto nitrocellulose-covered slides (Schott Nexterion NC-C, Jena, Germany) with a dedicated arrayer (2470 Arrayer, Aushon Biosystems, Billerica, MA). Five serial dilutions, ranging from 2 to 0.125 mg/ml, and 4 technical replicates per dilution were used for each sample. Detection was carried out with specific antibodies or without primary antibody (negative control) using an Autostainer Plus (Dako, Trappes, France). Briefly, slides were incubated with avidin, biotin, and peroxidase blocking reagents (Dako) and then saturated with TBS supplemented with 0.1% Tween 20 and 5% BSA (TBST-BSA). The slides were then probed by overnight incubation at 4 °C with primary antibodies diluted in TBST-BSA. The arrays were washed in TBST and then probed with horseradish peroxidase–coupled secondary antibodies (Jackson ImmunoResearch, Newmarket, UK) diluted in TBST-BSA for 1 hour at room temperature. The signal was amplified by incubating the slides with amplification reagent (Bio-Rad) for 15 minutes at room temperature. The arrays were then washed with TBST, probed with Cy5-streptavidin (Jackson ImmunoResearch) diluted in TBST-BSA for 1 hour at room temperature, and washed again in TBST. Total protein staining was achieved by incubating the arrays for 15 minutes in 7% acetic acid and 10% methanol, rinsing twice in water, incubating for 10 minutes in Sypro Ruby (Invitrogen), and rinsing again. The processed slides were dried by centrifugation and scanned with a GenePix 4000B microarray scanner (Molecular Devices, Sunnyvale, CA). Spot intensity was determined with MicroVigene 4.0.0.0 software (VigeneTech Inc., Carlisle, MA). Quantification of the data was achieved with SuperCurve [18], and the data were normalized against negative control slides and Sypro Ruby slides.

Statistical Analysis

Statistical analysis was performed using R v2.15.1 (http://www.cran.r-project.org). The tests were two-sided, with a type I error set at $\alpha = 0.05$. The study of relation between quantitative parameters was explored by Pearson or Spearman correlation coefficients according to statistical distribution. To identify makers differentially expressed (i) between *in vitro* and *in vivo* conditions and (ii) between the two groups of models, Mann-Whitney test was performed according to sample size and if assumptions of parametric test are not met. To highlight the most robust changes, studied markers were considered to be differentially accumulated when (i) Mann-Whitney test was significant ($P < .05$) and (ii) the change was more than 1.5-fold (fold change > 1.5). An arbitrary 1.5-fold change cutoff value means a minimum of 50% of variation in the 2 groups compared. To explore changes between the three sets of data obtained for U87MG model, Kruskal-Wallis test was performed followed by Dunn test for pairwise comparisons (adjustment according to the Dunn-Sidak correction). Hierarchical clustering of the data was performed on expression markers for each replicate or mean to build dendograms (Ward method). Heat maps were drawn using Gplots library.

Results

Global Similarity between Each Cell Line and Its Respective Xenograft

We performed a targeted proteomics approach using RPPA to study how similar the xenograft models are to their respective cell cultures. A total of 160 samples were analyzed: 14 cell lines (5 replicate extracts per cell line) and corresponding subcutaneous xenografts (2 fragments per tumor from 3 tumors). Each sample was printed in five serial dilutions and four technical replicates per dilution. Arrays were labeled with a selection of 89 highly specific antibodies: 39 against total proteins, 26 against phosphoproteins, and 24 ratios of phosphoproteins on total proteins were analyzed. The selected proteins and modifications are involved in 10 different signaling pathways: DNA repair, PI3K pathway, apoptosis, tyrosine kinase signaling, stress signaling, cell cycle, MAPK/ERK signaling, SAPK/JNK signaling, NFκB signaling, and adhesion/cytoskeleton (Table S1).

Firstly, we checked for the similarity between biological replicates, that is, between the five replicates for each cell line and between the six different fragments for each xenograft (two fragments per tumor from three different mice). For this, the Pearson correlation for each possible comparison was calculated for *in vitro* and *in vivo* samples. The mean correlations between *in vitro* replicates ranged from 0.82 to 0.97 and from 0.81 to 0.95 for *in vivo* replicates. The calculated standard error of the mean correlations is low (range 0.01-0.03), strengthening the high similarity among independent biological replicates. We also calculated the coefficient of variation (CV) for each sample to evaluate the variability between the biological replicates. This median CV ranged from 7% to 22% with a median of 12.6%. This again points to a very good similarity between the biological replicates. As expected, the CV was higher for *in vivo* replicates than for *in vitro* replicates.

Then, to evaluate the similarity of data obtained *in vitro* (cell culture) and *in vivo* (subcutaneous xenograft), we evaluated the correlation of RPPA signal in each paired model independently. As shown in Table 1, each cell culture-xenograft paired data were statistically correlated, with Pearson correlation coefficients higher than 0.7 for 12 of the 14 pairs. The SNB19 model is the most divergent between *in vitro* and *in vivo* conditions (correlation

Table 1. Comparison of *In Vitro* and *In Vivo* Data for Each Model

Cell Line	Cell Origin	Correlation between *In Vitro* and *In Vivo*[†]	Number of Proteins Differentially Expressed[§] and with a Fold Change > 1.5
SNB19	Glioblastoma	.27[‡]	27
CB193	Glioma grade III	.51[‡]	18
MO59K	Glioblastoma	.70[‡]	16
U118MG	Glioblastoma	.72[‡]	11
LU1205	Melanoma	.73[‡]	14
SF763	Glioblastoma	.74[‡]	13
U87MG	Glioblastoma	.77[‡]	37
SF767	Glioblastoma	.80[‡]	11
Hep2	Head and neck carcinoma	.81[‡]	11
T98G	Glioblastoma	.84[‡]	15
SK28	Melanoma	.86[‡]	6
HT29	Colon carcinoma	.87[‡]	0
U87MG/IC*	Glioblastoma	.89[‡]	1
HCT116	Colon carcinoma	.90[‡]	1
U251MG	Glioblastoma	.93[‡]	5

* Intracranial orthotopic xenograft.

† Pearson correlation.

‡ *P* value.

§ Mann-Whitney test ($P < .05$).

coefficient 0.27), whereas the U251MG model is the most conserved one (correlation coefficient 0.93). Altogether, these results highlight the fact that, at least for proteins explored in our study, there is a global similarity of protein expression and phosphorylation between cell culture and the corresponding subcutaneous xenograft model.

Four Pathways Highly Conserved Whatever the Cell Line Origin

To assess more in detail the stability of each protein expression and modification level between cell culture and its respective xenograft model (14 paired models), we evaluated the correlation of RPPA signals obtained for each studied marker independently. We found that 29 markers are highly conserved between *in vitro* and *in vivo* conditions (Pearson test $P < .05$) with a correlation ranging from 0.54 to 0.92 (Table 2). The *P* values were then adjusted for multiple testing using the Sidak correction, which decreased the number of conserved markers to 11. Akt, EGFR, NFkB, IKK β, and Vimentin showed very stable protein expression and phosphorylation levels between cell culture and subcutaneous xenograft models whatever the model. These proteins clearly highlight 4 of 10 explored signaling pathways: PI3K pathway, tyrosine kinase signaling, NFκB signaling, and adhesion/cytoskeleton. After Sidak correction, none of the proteins involved in DNA repair and stress signaling were found to be statistically conserved when comparing the 14 xenografts and their respective cell culture of origin. However, their conservation was heterogeneous among each cell culture-xenograft pair.

Eight of the 14 Cell Culture-Xenograft Pairs Cluster Together

To further visualize how similar or dissimilar xenografts were compared with their original cell line, we performed unsupervised hierarchical clustering analysis of RPPA data (Figures 1 and S.1). By looking at whether xenografts and cell culture pairs cluster together or not in the dendrogram, we identified three main groups named as *dissimilar group* (SNB19, MO59K, LU1205, CB193, U118MG, U87MG), *near-similar group* (HT29, HCT116, SF763, Hep2), and *highly similar group* (SK28, SF767, T98G, U251MG). For the models in the highly similar group, xenografts and cell lines cluster together, whereas for the models in the dissimilar group, they cluster far from each other. The models in the near-similar group show close, but not perfect, clustering. As expected, five of the six cell culture-xenograft pairs of *dissimilar group* were also the ones showing lower levels of correlation between cell culture and xenograft (correlation coefficients < 0.73).

We then determined the proteins that were differentially expressed between each cell line-xenograft pairs among the 65 tested markers (Table 1). We only considered significant proteins showing at least a 1.5-fold change in expression to focus on the biologically most relevant changes [19]. In the pairs from the *highly similar* and the *near-similar groups*, a mean of 9 and 6 markers, respectively, was statistically differentially expressed between the xenograft and the cell line, whereas a mean of 21 markers was identified in the pairs from the *dissimilar group*. In all three groups, the identified markers were extremely inconsistent and seem to be specific of each cell culture-xenograft pair.

We thus conclude that proteins whose expression is highly conserved between cell lines and xenografts are mostly related to Akt, NFkB, EGFR, and Vimentin, whereas the proteins that significantly change upon engraftment are more diverse.

Prediction of Cell Culture-Xenograft Pair Clustering by In Vitro Proteic Signature Analysis

Next, we wished to assess whether it is possible to identify those cell cultures that, upon engraftment, represent a relevant model, that is, a xenograft that closely resembles the cell line of origin in terms of protein expression. For this, we performed an unsupervised hierarchical clustering analysis of *in vitro* data only (Figure 2).

Interestingly, we observed two main clusters of cell cultures. The first corresponds to the *dissimilar group*, and the second combines the *near-similar* and *highly similar groups*. We studied the proteins that are differentially expressed between these three groups among cell cultures (Figure S.2). We observed few differences between the *near-similar* and the *highly similar groups*, whereas the *dissimilar group* is more distinct. Because the *near-similar* and *highly similar groups* here appeared as one single cluster in the *in vitro* data and showed few proteic differences, we hereafter called this the *similar group*. This suggests that a different pattern of protein exists between the cell cultures that will give rise to a similar xenografts compared with those that will give rise to a less conserved xenograft. We then explored which proteins were differentially expressed between these two groups of cell lines to identify potential predictive biomarkers. A Mann-Whitney test revealed that 11 of 65 proteins or phosphoproteins (Figures 3 and 4) are significantly differentially expressed between the two *in vitro* identified groups ($P < .05$). We observed two major relevant variations (fold change >1.5) for PTEN and Vimentin expression. PTEN expression was increased in the *similar group* (increased fold change of 1.8). In agreement with this increase of PTEN signaling, we observed a downward trend of Akt-Thr308 and Akt-S473 phosphorylations (decreased fold change of 1.2 and 1.3, respectively). Vimentin expression was severely reduced in the *similar group* (decreased fold change of 2.4) compared with the *dissimilar group*. Furthermore, we could indicate that phosho-H2AX and Rad21 seemed to be higher in the *similar group* (increased fold change of 1.4 for both). Expression of HSP90β, FEN1, integrin β4, MGMT, and EGFR was also slightly increased in the *similar group*. In conclusion, when a cell culture has low Akt and vimentin signaling levels and relatively high DNA damage response, its engraftment is more likely to produce a xenograft that is similar to the original cell culture.

Table 2. Conserved Proteins between *In Vitro* and *In Vivo* Whatever the Cell Line Origin

Name	Type	Description	Pearson Correlation	*P* Values	*P* Values after Sidak Adjustment
Phospho-Vimentin (Ser 459) on Vimentin	Phosphoprotein/protein	Cytoskeleton	0.92	<.001	<.001
Vimentin	Protein	Cytoskeleton	0.91	<.001	<.001
Phospho-Akt (Thr308) on Akt	Phosphoprotein	PI3K pathway	0.89	<.001	<.01
Phospho-Akt (Ser473) on Akt	Phosphoprotein	PI3K pathway	0.89	<.001	<.01
IKK β	Protein	NF-kB signaling	0.86	<.001	<.01
EGFR	Protein	Tyrosine kinase signaling	0.86	<.001	<.01
Phospho-EGFR (Thr669)	Phosphoprotein	Tyrosine kinase signaling	0.84	<.001	<.05
NF-kB p65	Protein	NF-kB signaling	0.83	<.001	<.05
Phospho-EGFR (Thr669) on EGFR	Phoshoprotein/protein	Tyrosine kinase signaling	0.82	<.001	<.05
Akt	Protein	PI3K pathway	0.81	<.001	<.05
Phospho-NF-kB p65 (Ser536) on NF-kB p65	Phoshoprotein/protein	NF-kB signaling	0.81	<.001	<.05
Src	Protein	Tyrosine kinase signaling, SRC family	0.79	<.001	NS
Phospho-Akt (Ser473)	Phosphoprotein	PI3K pathway	0.76	<.01	NS
Phospho-EGFR (Tyr 1173) on EGFR	Phoshoprotein/protein	Tyrosine kinase signaling	0.68	<.01	NS
Phospho-HSP27 (Ser82)	Phosphoprotein	Stress signaling, MAPK/ERK signaling	0.68	<.01	NS
Hsp90 β	Protein	Stress signaling	0.66	<.05	NS
PARP	Protein	DNA repair, apoptosis	0.64	<.05	NS
JunB	Protein	SAPK/JNK pathway	0.64	<.05	NS
FoxO3a/FKHRL1	Protein	Stress signaling, PI3K pathway, cell cycle	0.63	<.05	NS
Phospho-Akt (Thr308)	Phosphoprotein	PI3K pathway	0.62	<.05	NS
Cleaved PARP on PARP	Phoshoprotein/protein	DNA repair, apoptosis	0.62	<.05	NS
Phospho-Chk1 (Ser280) on Chk1	Phoshoprotein/protein	DNA repair, cell cycle	0.61	<.05	NS
Integrin β4	Protein	Cytoskeleton, adhesion	0.6	<.05	NS
Phospho-JunB on JunB	Phoshoprotein/protein	SAPK/JNK pathway	0.59	<.05	NS
VCP	Protein	DNA repair, cell cycle, apoptosis	0.59	<.05	NS
FAK	Protein	Tyrosine kinase signaling, adhesion	0.58	<.05	NS
Phospho-FAK (Tyr861) on FAK	Phoshoprotein/protein	Tyrosine kinase signaling, adhesion	0.57	<.05	NS
Phospho-histone H2AX (Ser139) on H2AX	Phoshoprotein/protein	DNA repair, chromatin	0.56	<.05	NS
Phospho-FAK (Tyr925) on FAK	Phoshoprotein/protein	Tyrosine kinase signaling, adhesion	0.54	<.05	NS

NS, not significant.

U87MG Cell Culture Is Closer to Intracranial Xenograft than to Subcutaneous Xenograft

U87MG is one of the most frequently used models for testing therapies for malignant gliomas [20]. This cell line was therefore assessed through a third model orthotopically engrafted. RPPA signal of U87MG cell culture model was compared with U87MG subcutaneous xenograft model but also with U87MG intracranial xenograft model. The proteins explored in this study were globally conserved between the three U87MG models (correlation coefficient 0.77-0.89, Table 1). However, hierarchical clustering reveals that the cell culture model seems to be closer to intracranial model than to subcutaneous model (Figure 1).

To decipher the differences in protein expression and phosphorylation between these three conditions, a Kruskall and Wallis test followed by a Dunn test adjusted by Sidak method was done using all replicates. In agreement with data presented in Table 1 and taking into account only fold changes >1.5, subcutaneous xenograft differentially expressed 37 and 32 markers compared with cell culture and intracranial xenograft respectively, whereas only 1 marker was differentially expressed between cell culture and intracranial xenograft

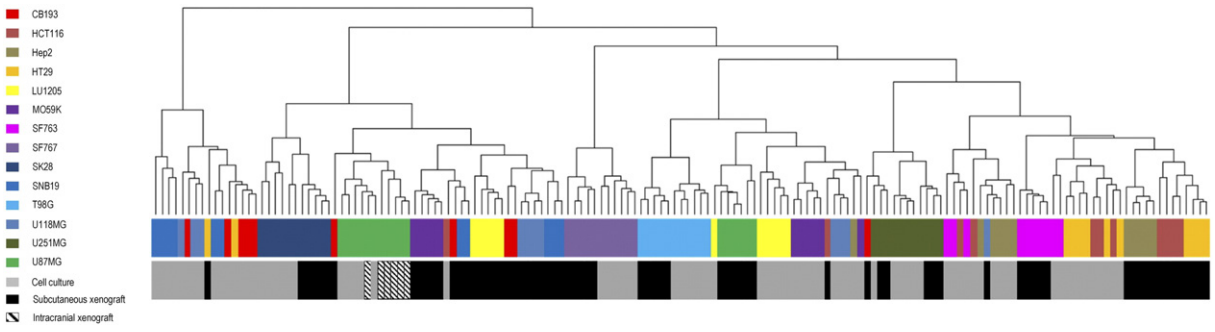

Figure 1. Hierarchical clustering of all data (cell line and xenograft).We explored a total of 89 proteic markers: 39 total proteins, 26 phosphoproteins, and 24 ratios of phosphoproteins on total proteins (Table S1). These proteins and modifications were chosen as representative of DNA repair, PI3K pathway, apoptosis, tyrosine kinase signaling, stress signaling, cell cycle, MAPK/ERK signaling, SAPK/JNK signaling, NFκB signaling, and adhesion/cytoskeleton. Data obtained for 14 cell lines were analyzed with 5 replicates for cell cultures and 6 replicates for subcutaneous xenograft models. For U87MG, an additional orthotopic model (six replicates) was studied. The dendrogram was built using Ward method.

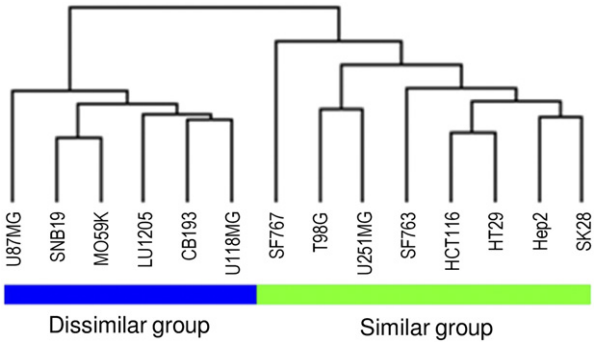

Figure 2. Hierarchical clustering of *in vitro* data.The mean values obtained for each explored protein or phosphoprotein for the 14 cell lines were used to build the dendrogram (Ward method). The first cluster corresponds to the *dissimilar group*. The second combines the *near-similar* and *highly similar groups*, called here the *similar group*.

model, underlining again the high similarity between these two models for the proteins assessed in this study.

Discussion

Human cancer-derived cell cultures and xenograft tumors are widely used models in cancer biology and innovative therapeutic studies [3]. There is a growing effort to reduce animal studies and find replacement methods to analyze and predict the effects of new treatments [21]. One alternative model proposed is the use of cell line cultures. Although it cannot replace all the information generated by animal models such as the pharmacokinetics and pharmacodynamics parameter or the impact of angiogenesis and inflammatory response on tumor growth, cell line studies might provide important information on intrinsic sensitivity of tumor cells to specific treatments. However, changes induced by the growth environment on the main constituents of the signaling pathways and constitutive stress response could alter the capacity of tumor cells to respond to treatment. Therefore, identifying markers to select cell lines and tumor models that do not differ should facilitate the study of the treatment effects and their mechanisms. Several elements could affect the transfer and extrapolation of *in vitro* results to *in vivo* experiments. Among them, the stability of tumor cells and xenograft phenotypes could be a major pitfall. Our objective in this study was to determine if expression and activation of proteins were involved in DNA repair, PI3K pathway, apoptosis, tyrosine kinase signaling, stress signaling, cell cycle, MAPK/ERK signaling, SAPK/JNK signaling, NFκB signaling, and adhesion/cytoskeleton.

We chose the RPPA technology to study these proteins of interest because it requires only a few micrograms of protein lysate to study activation of cell signaling pathways, and allows comparing hundreds of samples in the same experiment. We could thus include replicate samples for the cell lines and different tumor regions from multiple mice for the xenografts to obtain robust data and assess heterogeneity within and among tumors.

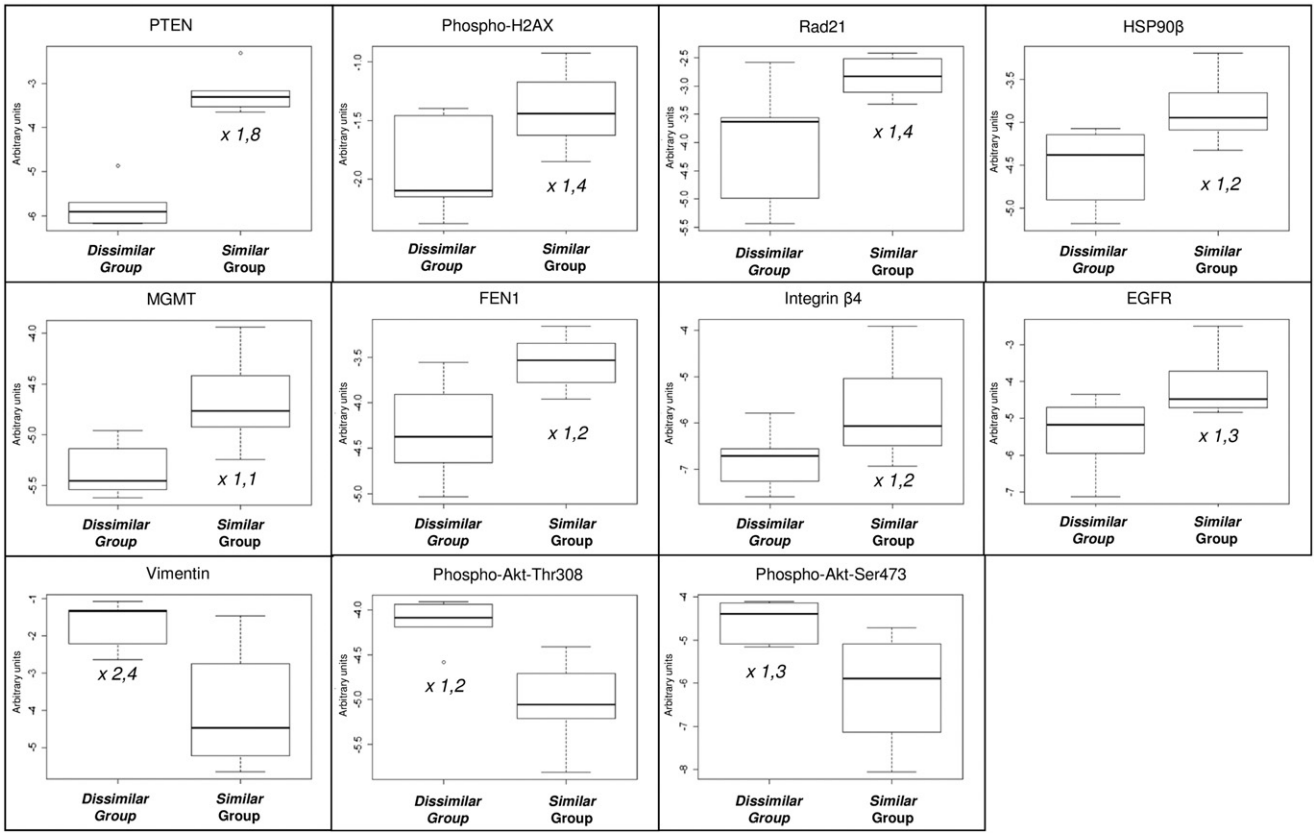

Figure 3. Differentially expressed proteins between similar and dissimilar groups.Among the proteic markers explored, Mann-Whitney test was performed ($P < .05$) to identify makers differentially expressed between the two groups of models. Boxplots for identified markers and fold change between *similar* and *dissimilar groups* are indicated.

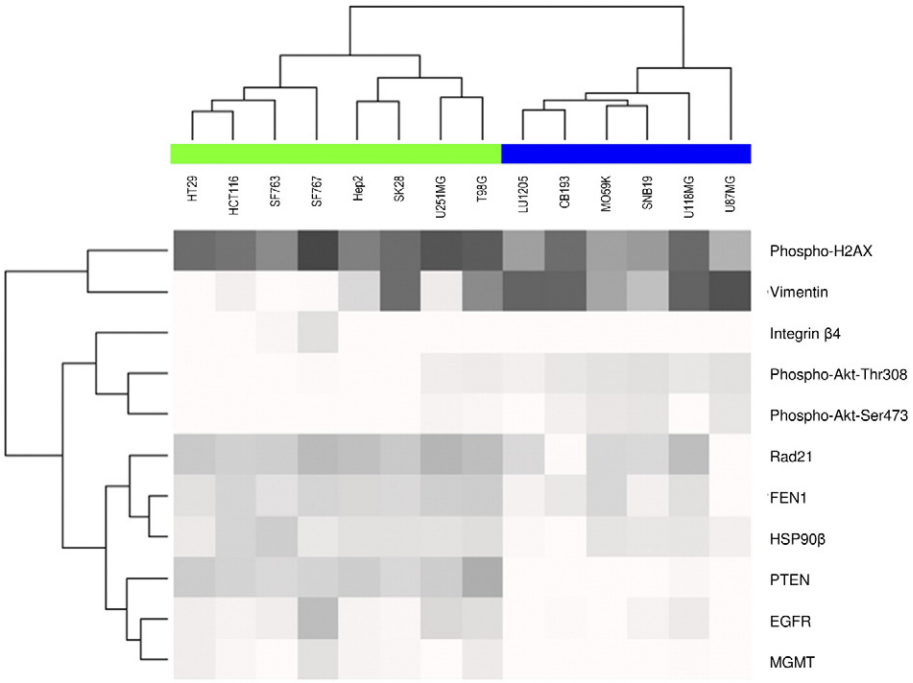

Figure 4. Heat map of differentially expressed proteins between similar and dissimilar groups.Expression range from low (white) to high (black) for the 11 differentially expressed markers between the *similar (green)* and *dissimilar* groups *(blue)*.

We found a high level of reproducibility of RPPA analysis for replicates both *in vitro* and *in vivo In vitro* reproducibility was quite expected. The high homogeneity *in vivo* between different areas of the tumor or different tumors indicates that, in these xenograft models, the tumors are relatively homogeneous, a characteristic that facilitates the interpretation of the data but might not reflect the status of all patient tumors [3].

We also found a global similarity between cell cultures and their paired xenograft regarding protein expression. Twelve out of 14 pairs had a correlation coefficient superior to 0.7. Furthermore, a detailed analysis revealed that Akt, EGFR, NFkB, IKK β, and Vimentin showed very stable protein expression and phosphorylation levels between cell culture and subcutaneous xenograft models whatever the model. These proteins clearly highlight 4 of 10 explored signaling pathways: PI3K pathway, tyrosine kinase signaling, NFκB signaling, and adhesion/cytoskeleton.

Gathering evidence has revealed that Akt [22–25] and NF-κB [26,27] signaling pathways play an important role in cancer progression, aggressiveness, and resistance to treatment and therefore represent potential target to improve current treatments. EGF signaling alterations, and especially its receptor mutation that increases intracellular signaling, are a major issue in cancer research over the last decade [28–33]. Vimentin, the major intermediate filament of mesenchymal cells, is often used as a marker of mesenchymally derived cells or cells undergoing an epithelial-to-mesenchymal transition (EMT) during both normal development and metastatic progression [34]. The high conservation of these four pathways during engraftment suggests that these pathways are of importance for the tumor and that they might not be directly influenced by their environment. All other proteins, including DNA repair proteins, were heterogeneously conserved depending on the cell line. This finding suggests that for specific studies on specific proteins with targeted therapies, extrapolation results from monolayer cultures to xenografts should be cautiously assessed. These differences could account for discrepancies sometime reported between cell response to treatment and results *in vivo* [1,3]. One of the major differences between the cell cultures in monolayer and tumors is the presence of infiltrating cells (stroma). Not only are these cells purified with the tumor cells in the tumor and could alter the protein pattern, but according to their nature, they can differently affect the tumor cells. The similarity of the cell cultures with the tumors in the majority of the models indicates that these infiltrating cells represent only a minor fraction of the tissue and did not affect the tumor cells. Indeed, histological analyses of the tumors (data not shown) have described all studied xenografts as homogeneous masses of cancer cells with minimal stromal infiltration. The percentage of tumor cells has been evaluated to be more than 80% for all xenografts with no differences found between groups.

We also identified, after unsupervised hierarchical clustering analysis of RPPA signal, two clusters of cell lines, for which data from cell culture and subcutaneous xenograft are either similar or not. We further studied the factors that differentiate these two groups of cell lines. We found that cell lines harboring a high level of vimentin and a low level of PTEN concurrently with a high Akt pathway activation gave rise to xenografts that were less similar to the original cell line, probably because they were more sensitive to the environment change. These proteins are associated with EMT [35]. EMT is a critical event in the induction of cell motility and increased cell survival under physiological situations like wound healing or development as well as during invasion and metastasis. Vimentin is an intermediate filament protein which is characteristically upregulated in cells undergoing EMT. For decades, vimentin has been considered as a marker for EMT, and recent studies support the notion that vimentin is a prerequisite for EMT induction. Our results thus

suggest that cell lines having EMT features produce less reliable xenografts. Validation of these findings would require a larger series of cell lines and xenograft models and should include more markers of EMT.

In the *near-similar* and *highly similar groups*, five out of eight models are PTEN wild type, whereas all models in the *dissimilar group* are mutated for PTEN [36–40]. When we look individually at each model, there is no clear correlation between mutation status and protein level. All wild-type samples express high levels of PTEN, but mutant samples can express either high or low levels of PTEN. This probably depends on the type of mutation (deletion, truncating, or missense) and the localization of the mutation relative to the antibody epitope (which is C-terminal). When taken together, the models with mutant PTEN express globally lower levels of protein compared with wild type (P = .02). The difference that we observed between the *near-similar/highly similar* and the *dissimilar groups* in terms of PTEN levels thus probably reflects the mutation status. It would be interesting to address in a larger panel of models whether PTEN mutation status by itself can predict the stability of xenograft models.

Another unexpected result that this study highlighted was the effect of the tumor location on the protein markers. U87MG model is a widely used glioblastoma model that was established from a female glioblastoma patient [20]. Here, we have studied the similarity in protein expression between three different conditions: monolayer cell culture, subcutaneous xenograft, and orthotopic (brain) xenograft. Orthotopic xenograft models, although technically more challenging, are often preferred as an advanced step in drug development or biological studies [2]. Interestingly, we have shown that, in terms of protein expression, orthotopic U87MG xenograft was by far more similar to monolayer cell culture (correlation of 0.89 and cluster together) than the subcutaneous model. It would be interesting to confirm this in other cancer models grafted both subcutaneously and orthotopically.

Conclusion

Here we reported a global high conservation of protein expression and activation between cell culture and xenograft models. In particular, four pathways were found to be highly correlated among all cancer models: Akt, NFkB, EGFR, and Vimentin. Other proteins were heterogeneously conserved depending on the cell line. Cell line models with low activation of the Akt pathway and low expression of Vimentin seem to give rise to more stable xenografts. These results may be useful for the extrapolation of cell culture experiments to *in vivo* models notably in novel targeted drug discovery and biomarkers research.

Acknowledgements

We thank Aurélie Barbet and Lamine Coulibaly for performing the RPPA experiments. We are grateful to Sylvie Job-Troncale for initial RPPA data normalization and analysis.

Appendix A. Supplementary data

Supplementary data to this article can be found online at http://dx.doi.org/10.1016/j.tranon.2016.05.005.

References

[1] Hughes J, Rees S, Kalindjian S, and Philpott K (2011). Principles of early drug discovery. *Br J Pharmacol* **162**, 1239–1249.
[2] Stylli SS, Luwor RB, Ware TMB, Tan F, and Kaye AH (2015). Mouse models of glioma. *J Clin Neurosci* **22**, 619–626.
[3] Marx V (2014). Models: stretching the skills of cell lines and mice. *Nat Methods* **11**, 617–620.
[4] Hickman JA, Graeser R, de Hoogt R, Vidic S, Brito C, Gutekunst M, and van der Kuip H (2014). IMI PREDECT Consortium. Three-dimensional models of cancer for pharmacology and cancer cell biology: capturing tumor complexity in vitro/ex vivo. *Biotechnol J* **9**, 1115–1128.
[5] Gazdar AF, Girard L, Lockwood WW, Lam WL, and Minna JD (2010). Lung cancer cell lines as tools for biomedical discovery and research. *J Natl Cancer Inst* **102**, 1310–1321.
[6] Wilding JL and Bodmer WF (2014). Cancer cell lines for drug discovery and development. *Cancer Res* **74**, 2377–2384.
[7] Hayes DF (2015). Biomarker validation and testing. *Mol Oncol* **9**, 960–966.
[8] Henry NL and Hayes DF (2012). Cancer biomarkers. *Mol Oncol* **6**, 140–146.
[9] Gallagher RI and Espina V (2014). Reverse phase protein arrays: mapping the path towards personalized medicine. *Mol Diagn Ther* **18**, 619–630.
[10] van Otterdijk SD and Michels KB (2016). Transgenerational epigenetic inheritance in mammals: how good is the evidence? *FASEB J* **30**, 2457–2465.
[11] Imamura Y, Mukohara T, Shimono Y, Funakoshi Y, Chayahara N, Toyoda M, Kiyota N, Takao S, Kono S, and Nakatsura T, et al (2015). Comparison of 2D- and 3D-culture models as drug-testing platforms in breast cancer. *Oncol Rep* **33**, 1837–1843.
[12] Levin VA, Panchabhai S, Shen L, and Baggerly KA (2012). Protein and phosphoprotein levels in glioma and adenocarcinoma cell lines grown in normoxia and hypoxia in monolayer and three-dimensional cultures. *Proteome Sci* **10**, 5.
[13] He W, Kuang Y, Xing X, Simpson RJ, Huang H, Yang T, Chen J, Yang L, Liu E, and He W, et al (2014). Proteomic comparison of 3D and 2D glioma models reveals increased HLA-E expression in 3D models is associated with resistance to NK cell-mediated cytotoxicity. *J Proteome Res* **13**, 2272–2281.
[14] Olsen JV and Mann M (2013). Status of large-scale analysis of post-translational modifications by mass spectrometry. *Mol Cell Proteomics* **12**, 3444–3452.
[15] Sharma K, D'Souza RCJ, Tyanova S, Schaab C, Wiśniewski JR, Cox J, and Mann M (2014). Ultradeep human phosphoproteome reveals a distinct regulatory nature of Tyr and Ser/Thr-based signaling. *Cell Rep* **8**, 1583–1594.
[16] Masuda M and Yamada T (2015). Signaling pathway profiling by reverse-phase protein array for personalized cancer medicine. *Biochim Biophys Acta* **1854**, 651–657.
[17] Akbani R, Becker K-F, Carragher N, Goldstein T, de Koning L, Korf U, Liotta L, Mills GB, Nishizuka SS, and Pawlak M, et al (2014). Realizing the promise of reverse phase protein arrays for clinical, translational, and basic research: a workshop report: the RPPA (Reverse Phase Protein Array) Society. *Mol Cell Proteomics* **13**, 1625–1643.
[18] Troncale S, Barbet A, Coulibaly L, Henry E, He B, Barillot E, Dubois T, Hupé P, and de Koning L (2012). NormaCurve: a SuperCurve-based method that simultaneously quantifies and normalizes reverse phase protein array data. *PLoS One* **7**, e38686.
[19] Gujral TS, Karp RL, Finski A, Chan M, Schwartz PE, MacBeath G, and Sorger P (2013). Profiling phospho-signaling networks in breast cancer using reverse-phase protein arrays. *Oncogene* **32**, 3470–3476.
[20] Goldbrunner RH, Wagner S, Roosen K, and Tonn JC (2000). Models for assessment of angiogenesis in gliomas. *J Neurooncol* **50**, 53–62.
[21] Workman P, Aboagye EO, Balkwill F, Balmain A, Bruder G, Chaplin DJ, Double JA, Everitt J, Farningham DA, and Glennie MJ, et al (2010). Guidelines for the welfare and use of animals in cancer research. *Br J Cancer* **102**, 1555–1577.
[22] Chautard E, Ouédraogo ZG, Biau J, and Verrelle P (2014). Role of Akt in human malignant glioma: from oncogenesis to tumor aggressiveness. *J Neurooncol* , 1–11.
[23] Toren P and Zoubeidi A (2014). Targeting the PI3K/Akt pathway in prostate cancer: challenges and opportunities (review). *Int J Oncol* **45**, 1793–1801.
[24] Wilks ST (2015). Potential of overcoming resistance to HER2-targeted therapies through the PI3K/Akt/mTOR pathway. *Breast Edinb Scotl* **24**, 548–555.
[25] Stegeman H, Span PN, Kaanders JHAM, and Bussink J (2014). Improving chemoradiation efficacy by PI3-K/AKT inhibition. *Cancer Treat Rev* **40**, 1182–1191.
[26] Escárcega RO, Fuentes-Alexandro S, García-Carrasco M, Gatica A, and Zamora A (2007). The transcription factor nuclear factor-kappa B and cancer. *Clin Oncol* **19**, 154–161.
[27] Liu F, Bardhan K, Yang D, Thangaraju M, Ganapathy V, Waller JL, Liles GB, Lee JR, and Liu K (2012). NF-κB directly regulates Fas transcription to modulate Fas-mediated apoptosis and tumor suppression. *J Biol Chem* **287**, 25530–25540.

[28] Mok TS, Wu Y-L, Thongprasert S, Yang C-H, Chu D-T, and Saijo N, et al (2009). Gefitinib or carboplatin-paclitaxel in pulmonary adenocarcinoma. *N Engl J Med* **361**, 947–957.

[29] Fukuoka M, Wu Y-L, Thongprasert S, Sunpaweravong P, Leong S-S, and Sriuranpong V, et al (2011). Biomarker analyses and final overall survival results from a phase III, randomized, open-label, first-line study of gefitinib versus carboplatin/paclitaxel in clinically selected patients with advanced non-small-cell lung cancer in Asia (IPASS). *J Clin Oncol* **29**, 2866–2874.

[30] Rosell R, Carcereny E, Gervais R, Vergnenegre A, Massuti B, and Felip E, et al (2012). Erlotinib versus standard chemotherapy as first-line treatment for European patients with advanced EGFR mutation-positive non-small-cell lung cancer (EURTAC): a multicentre, open-label, randomised phase 3 trial. *Lancet Oncol* **13**, 239–246.

[31] Zhou C, Wu YL, Chen G, Feng J, Liu X-Q, and Wang C, et al (2015). Final overall survival results from a randomised, phase III study of erlotinib versus chemotherapy as first-line treatment of EGFR mutation-positive advanced non–small-cell lung cancer (OPTIMAL, CTONG-0802). *Ann Oncol* **26**, 1877–1883.

[32] Bonner JA, Harari PM, Giralt J, Cohen RB, Jones CU, Sur RK, Raben D, Baselga J, Spencer SA, and Zhu J, et al (2010). Radiotherapy plus cetuximab for locoregionally advanced head and neck cancer: 5-year survival data from a phase 3 randomised trial, and relation between cetuximab-induced rash and survival. *Lancet Oncol* **11**, 21–28.

[33] Jonker DJ, O'Callaghan CJ, Karapetis CS, Zalcberg JR, Tu D, Au H-J, Berry SR, Krahn M, Price T, and Simes RJ, et al (2007). Cetuximab for the treatment of colorectal cancer. *N Engl J Med* **357**, 2040–2048.

[34] Satelli A and Li S (2011). Vimentin in cancer and its potential as a molecular target for cancer therapy. *Cell Mol Life Sci* **68**, 3033–3046.

[35] Kalluri R and Weinberg RA (2009). The basics of epithelial-mesenchymal transition. *J Clin Invest* **119**, 1420–1428.

[36] Huang X, Zhang Y, Tang Y, Butler N, Kim J, Guessous F, Schiff D, Mandell J, and Abounader R (2013). A novel PTEN/mutant p53/c-Myc/Bcl-XL axis mediates context-dependent oncogenic effects of PTEN with implications for cancer prognosis and therapy. *Neoplasia* **15**, 952–965.

[37] Xing F, Persaud Y, Pratilas CA, Taylor BS, Janakiraman M, and She Q-B, et al (2012). Concurrent loss of the PTEN and RB1 tumor suppressors attenuates RAF dependence in melanomas harboring (V600E)BRAF. *Oncogene* **31**, 446–457.

[38] Furnari FB, Lin H, Huang HS, and Cavenee WK (1997). Growth suppression of glioma cells by PTEN requires a functional phosphatase catalytic domain. *Proc Natl Acad Sci U S A* **94**, 12479–12484.

[39] Millet P, Granotier C, Etienne O, and Boussin FD (2013). Radiation-induced upregulation of telomerase activity escapes PI3-kinase inhibition in two malignant glioma cell lines. *Int J Oncol* **43**, 375–382.

[40] Paraiso KHT, Haarberg HE, Wood E, Rebecca VW, Chen YA, and Xiang Y, et al (2012). The heat shock protein-90 inhibitor XL888 overcomes BRAF inhibitor resistance mediated through diverse mechanisms. *Clin Cancer Res* **18**, 2502–2514.